Christoph Geers
Swiss Nanoanalytics
Adolphe Merkle Institute
Chemin des Verdiers 4
CH-1700 Fribourg

Prof. Alke Fink and Barbara Rothen-Rutishauser
Adolphe Merkle Institute
University of Fribourg
Chemin des Verdiers 4
CH-1700 Fribourg

Analysis Report

General Information

Customer Bundesamt für Gesundheit (BAG), Bern
Sabine Frey
Sektion Risikobeurteilung
Tel.: 058 463 79 99, E-Mail: sabine.frey@bag.admin.ch

Date of sample arrival 04.06.2020
Date of report Monday, August 03, 2020

Sample name	CAS Number	Internal ID
Nickel nanoparticles	1313-99-1	2020_001_S001
Titania nanoparticles	13463-67-7	2020_001_S002
Carbon black (Scream Ink Pitch Black)	1333-86-4	2020_001_S003
Carbon black (True Black Tattoo Ink)	1333-86-4	2020_001_S004
Gold nanoparticles	7440-57-5 (bulk)	2020_001_S005
Silver nanoparticles	7440-22-4 (bulk)	2020_001_S006
Titania nanoparticles (Sukgyung AT Co)	13463-67-7	2020_001_S007
4-([4-(Aminocarbonyl)phenyl]azo)-N-(2-ethoxyphenyl)-3-hydroxynaphthalene-2-carboxamide (Red Tattoo Ink)	2786-76-7	2020_001_S008

Operators Ana Milosevic, Christoph Geers
Report Christoph Geers, Ana Milosevic

Analytical methods

Nanoparticle dispersion
Comments:
Powder samples were dispersed according to the generic NANOGENOTOX dispersion protocol and the NANoREG SOP for probe-sonicator calibration of delivered acoustic power. Following the probe calibration and sonication (Branson SFX550 Digital Sonifier 550), samples were characterized immediately to mimic their exposure scenario. The exceptions were samples which were incubated for 48 h in cell culture media to assess their stability.
Further details regarding the sonication are listed in Annex I of this report

Transmission Electron Microscopy (TEM)
Comments:
Following the dispersion of the powder samples, the sedimentation behaviour was observed, which indicated sample aggregation/agglomeration. Due to the noticeable aggregation/ agglomeration of the samples and hence polydispersity, TEM sample preparation technique described in the NANoREG D2.10 SOP01 was not optimal. The "Grid on the drop" method shows bias towards smaller particles, while the "drop on the grid" method shows bias towards larger particles and aggregates/agglomerates. In order to obtain a representative TEM sample, a previously described technique was used (DOI: 10.1038/srep09793). Samples were prepared by depositing 5 µl of obtained dispersions on a grid (Formvar-coated 200 mesh copper grid) and were imaged the following day.
The imaging setup used consisted of a Tecnai Spirit - BioTwin lens | 120 kV LaB6 emitter equipped with a Veleta 2048x2048 camera. To set the optimal parameters for the sample imaging, the NANoREG D2.10 SOP 02 was followed, while for the image analysis the NANoREG D2.10 SOP 03, NANoREG D2.10 SOP 04 and NANoREG D2.10 SOP 05 were followed. To analyze the images, the EPFL ELN software was used.
Further details regarding the measurements are listed in Annex I, which is attached to this report.

Dynamic Light Scattering (DLS)
Comments:
Following the NANoREG SOP for nanoparticle dispersion, samples were diluted to the highest concentration used for the cell exposure studies (instructions provided by Givaudan). Namely, S001, S002, S007 and S008 dispersions were diluted down to 0.256 mg/mL, S005 and S006 was diluted 1:8 and 1:4 fold respectively, while S003 and S004 were diluted down to 0.4 mg/mL. For the DLS measurements all samples were too concentrated, except of S005 and S006, which were even as a stock solution already too diluted. High sample concentrations can lead to multiple light scattering events within the sample and thus skew DLS data, while low sample concentrations cannot be reliably measured, as a lack of a scattering signal can result in an unreliable correlation function leading to unreliable data.
For that reason, S001, S002, S007 and S008 were further diluted 10x, while S003 and S004, due to the strong interference with the laser light, had to be further diluted 1000x. The stock solutions of S005 and S006 were measured due to their low concentration, making a further dilution unnecessary.

DLS measurements were performed following the NANoREG D2.08 SOP 02 as close as that was possible, considering that the measurements were performed on a Brookhaven Z Sizer with a fixed angle of 90° as opposed to using a recommended Malvern ZetaSizer at an angle of 173°. Furthermore, samples were additionally analyzed with a 3D DLS by LS Instruments at angles of 37 °C and 90°.
Sample stability was assessed at 0 h and after 48 h following the incubation in 1% FBS DMEM + 1% DMSO as per instructions by Givaudan. The 48 h incubation was done at 37 °C. Samples were incubated at the highest concentration for the cell exposure, but analysed at the diluted concentrations due to the above mentioned limitations.
Further details regarding the measurements are listed in Annex I, which is attached to this report.

Endotoxin Analysis
Comments:
Due to the known interference of nanoparticles and potential difficulties when performing endotoxin assays, on recommendation from several past and ongoing EU projects, the analysis of samples was conducted via two different assays. Here the LAL Pierce Endotoxin Assay supplied by ThermoScientific and Endosafe® nexgen-PTS™ device provided by Charles River were used. According to the SOP and guidance documents from the European Nanomedicine Characterization Laboratory (EU NCL), USA Nanomedicine Characterization Laboratory (USA NCL) and Food and Drug Administration (FDA), the assay performance was assessed based on a standard curve accuracy, sample measurement precision and potential signal enhancement/inhibition effects. For the assay to qualify for a passing result, the R value of the standard curve has to be >0.98, and the accuracy and precision of each value have to be within 25% and the signal recovery has to be between 50-200%.
As previously stated, due to their interference with colorimetric assays, the nanoparticle samples have to be optimized to qualify for above described analysis. This is achieved by centrifugation (NANoREG D5_06_LAL protocol) and sample dilution. Samples were centrifuged at the highest concertation used for the cell exposure and diluted in a series down to the maximum valid dilution (MVD) (LAL. UPDATE. Volume 13, No. 4. December 1995). The negligible absorbance interference for the LAL Pierce Assay was observed at the MVD (10x) making the samples eligible for further analysis. Furthermore, due to the sensitivity of the Endosafe® nexgen-PTS™ device, samples could be diluted down to 100x, thus reducing the potential interference.
Once all above given conditions are met, the data qualified as reliable.
Both assays were performed according to the producers' instructions.

Analysis - Results

Nanoparticle dispersion

Comments:

Samples S001, S002, S007 and S008 were dispersed as described above. S001, S002 and S007 resulted in dispersions which showed signs of sedimentation over time, which was not clear for S008. Due to its faster observable sedimentation (when compared to S002 and S007) S001 was rapidly analyzed after the dispersion was made, in order to mimic the cell exposure procedure.

To better understand the sedimentation and its rate, time resolved UV-Vis measurements are advisable, while in order to produce stable dispersions, alternative, an optimized dispersion protocol is advisable.

It should be noted that due to the high concentration of the dispersions (2.56 mg/mL), sedimentation can often be observed only upon inspection of the vials' bottom, rather than via the side view. Only in the case of rapid sedimentation, such as was the case with S001, the sedimentation was clear even via the side view (Figure 1).

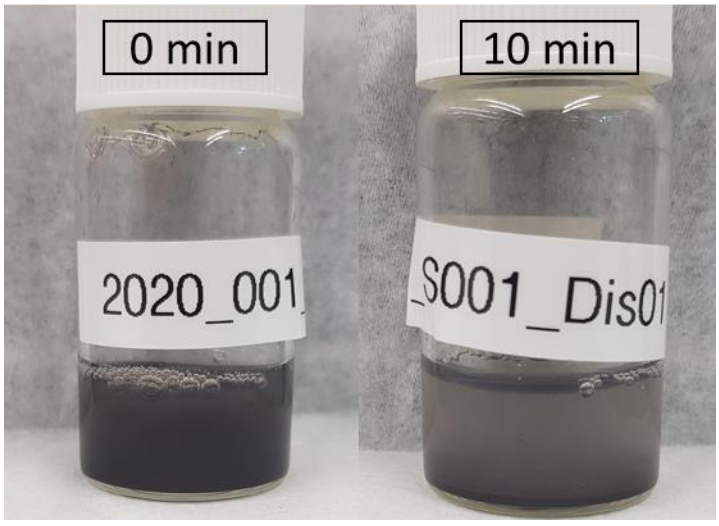

Figure 1: Overview of the S001 sample after dispersion (0 min and 10 min)

Transmission electron microscopy (TEM) and sizing analysis

Comments:

TEM images of nanoparticle dispersions were taken at minimum 10 randomized positions on the grid as per NANoREG D2.10 SOP 02. The summary of nanoparticle characterization is given in Table 1 and in the Annex I.

Due to the fact that most of the samples appeared to be aggregated/agglomerated, the ECD based size measurements are not applicable as aggregates/agglomerates cannot be assumed as spherical. For the aggregated samples, the Feret diameter offers a more accurate size estimate, which is why it was used for the analysis.

Significant variability in the data obtained for median, mean and mode of the nanoparticle size indicates that samples are polydisperse. Polydispersity and aggregation/agglomeration are also indicated by the broad range of measured sizes as shown in Table 1 and Figures 2-9. The only two samples without signs of aggregation/agglomeration, and a narrow size distribution, were S005 and S006. Those two samples are also the only two with apparent high sphericity, while the other samples, likely due to their aggregation/agglomeration appear as aggregates/agglomerates of various fractal dimensions (Table 2).

Table 1. TEM sizing - data summary

Sample name	Magnification (X)	Feret – size							
		Median Diameter		Mean Diameter		Mode Diameter		Range	
		nm	SD (nm)	nm	SD (nm)	Nm	SD (nm)	Min (nm)	Max (nm)
S001	1150	80.0	287.5	167.1	287.5	32.0	287.5	8	1968
S001	160000	22.5	35.3	34.5	35.3	24.3	35.3	4	264
S002	4200	822.2	1216.1	1377.5	1216.1	400.0	1216.1	178	4689
S002	43000	46.8	51.3	61.6	51.3	32.9	51.3	10	371
S003	20500	195.3	142.6	224.7	142.6	158.1	142.6	37	795
S004	9900	327.1	258.1	360.4	258.1	196.3	258.1	65.4	1654.2
S005	220000	5.8	1.0	6.0	1.0	5.8	1.0	1	9
S006	300000	6.7	2.2	7.1	2.2	5.2	2.2	1	12
S007	16500	91.4	172.1	168.3	172.1	51.4	172.1	11	1000
S008	20500	168.2	249.6	231.8	249.6	18.7	249.6	9.3	1392.5

Table 2. TEM - shape description summary. Representative particles are shown in the table.

Sample	Shape Description	Examples
S001	Spheroidal, Medium Sphericity, Sub-Angular	
S002	Ellipsoidal, Medium Sphericity, Sub-rounded	
S003	Ellipsoidal, Low Sphericity, Very Angular	
S004	Linear, Low Sphericity, Very Angular	
S005	Spheroidal, High Sphericity, Well-Rounded	
S006	Spheroidal, High Sphericity, Well-Rounded	
S007	Ellipsoidal, Low Sphericity, Angular	
S008	Ellipsoidal, Low Sphericity, Sub-Rounded	

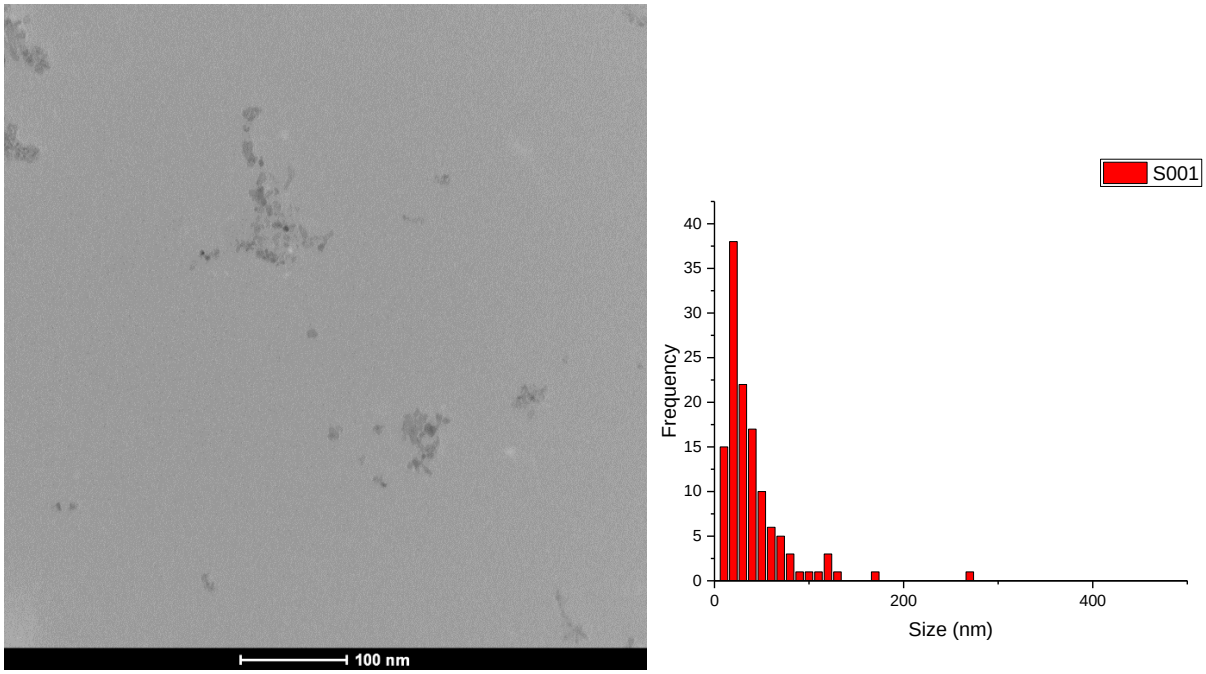

Figure 2: Representative TEM image of the S001 dispersion at the position 1 and the histogram representing the sample size and size distribution.

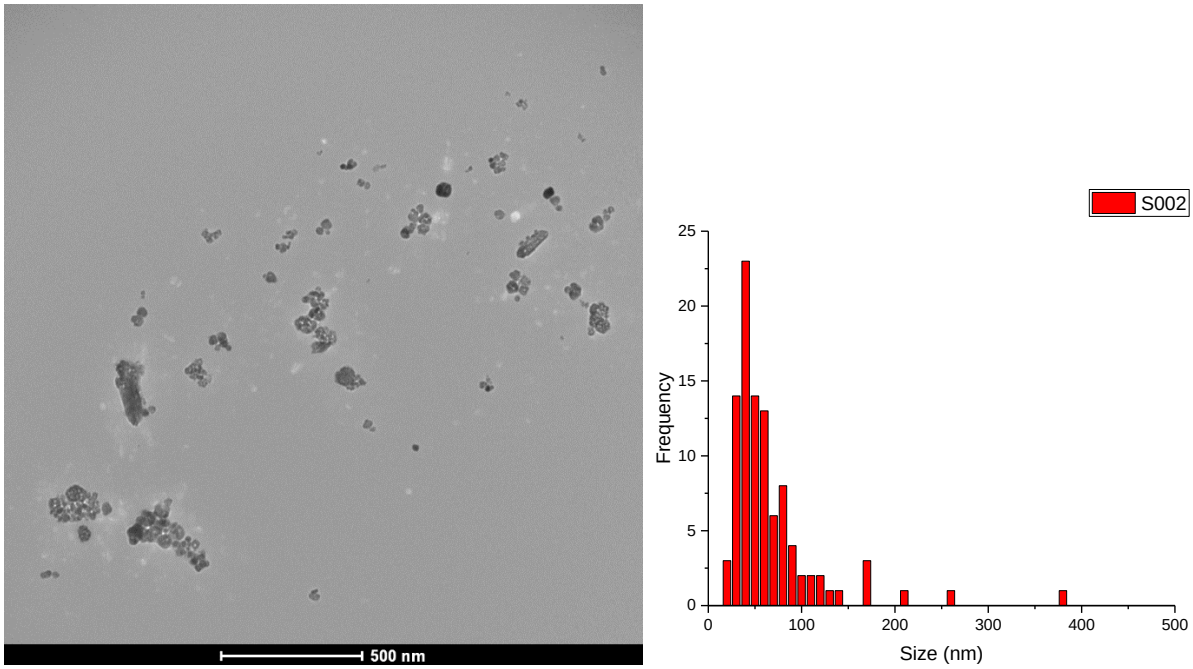

Figure 3: Representative TEM image of the S002 dispersion at the position 1 and the histogram representing the sample size and size distribution.

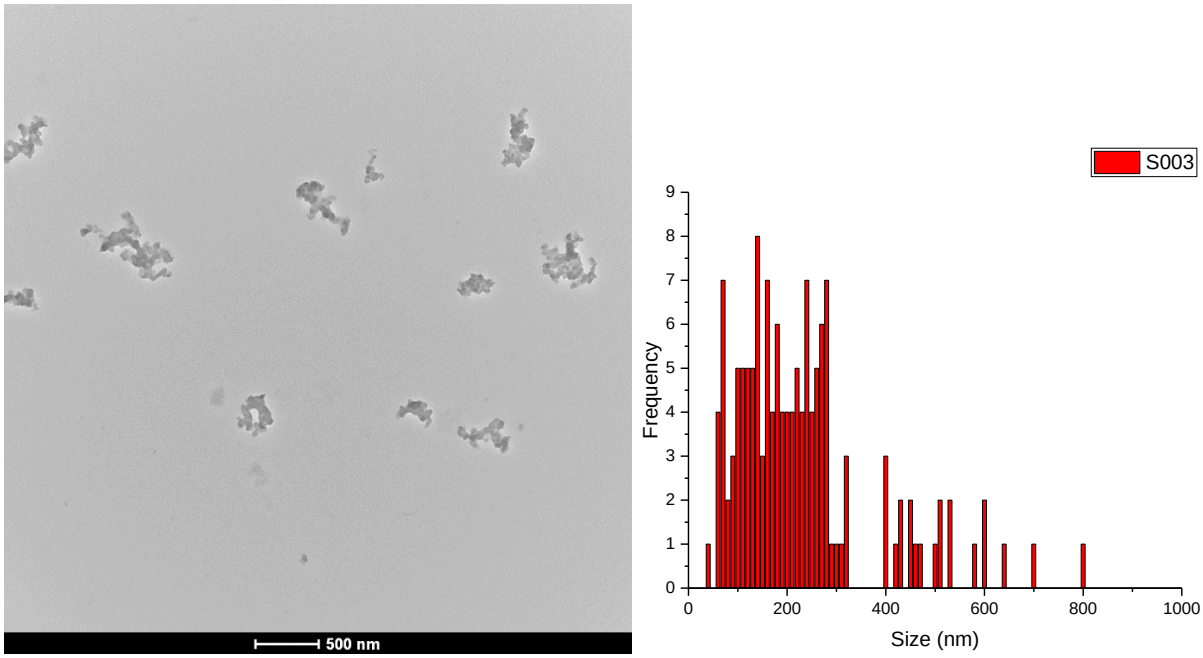

Figure 4: Representative TEM image of the S003 dispersion at the position 1 and the histogram representing the sample size and size distribution.

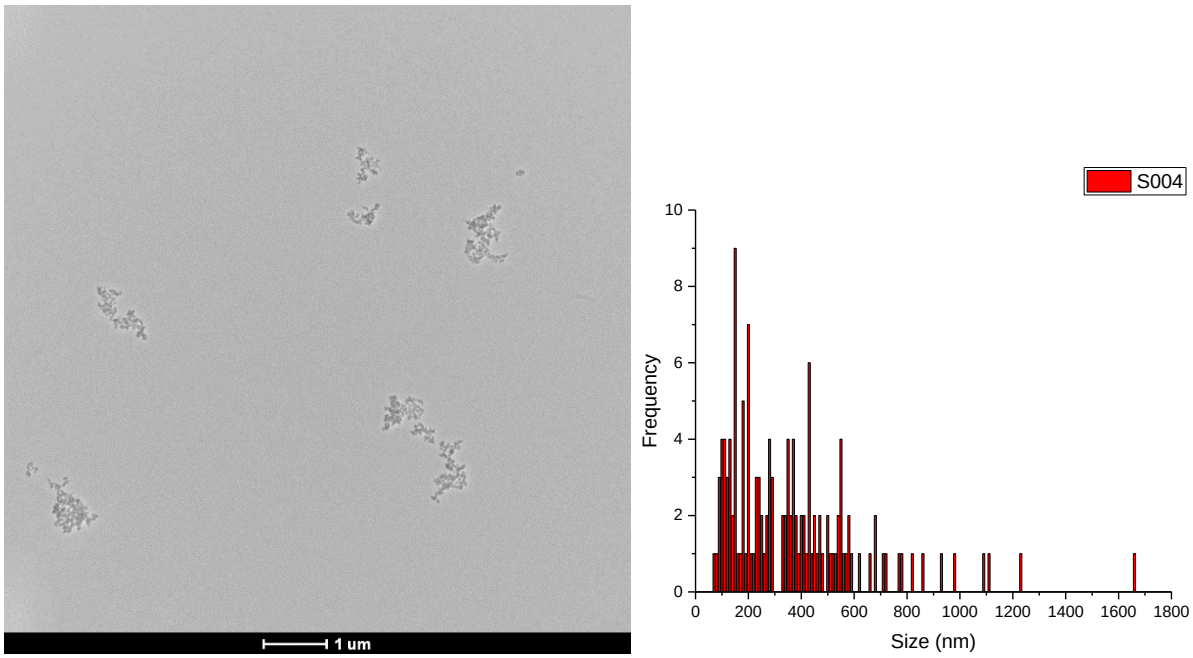

Figure 5: Representative TEM image of the S004 dispersion at the position 1 and the histogram representing the sample size and size distribution.

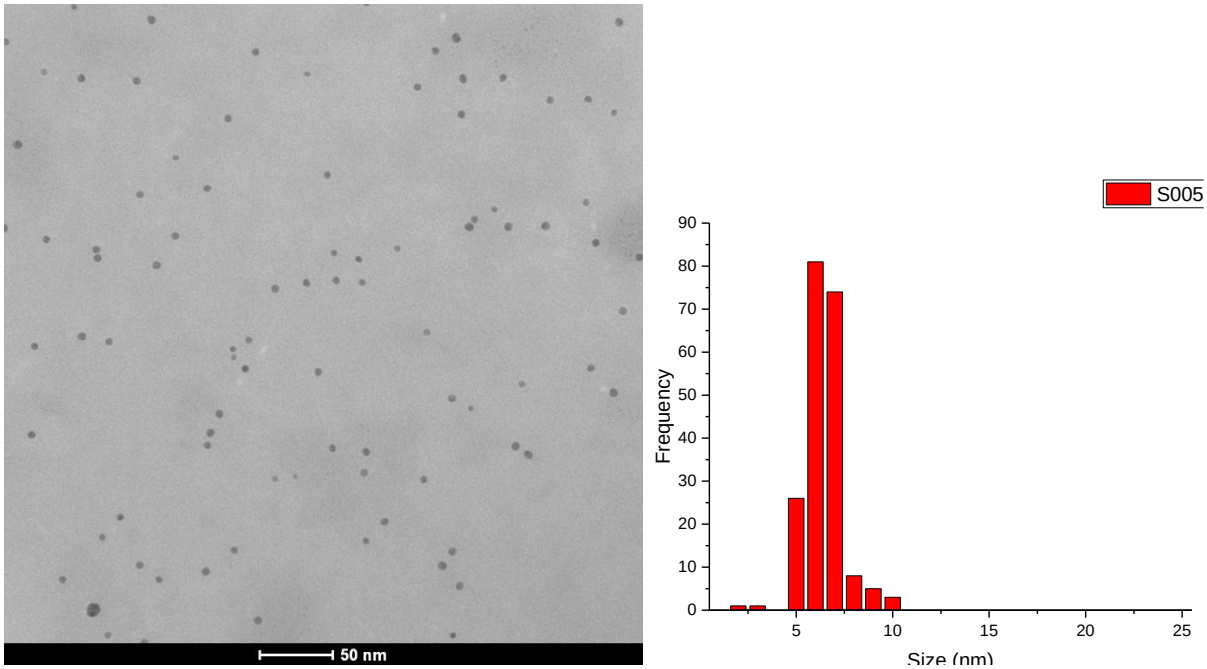

Figure 6: Representative TEM image of the S005 dispersion at the position 1 and the histogram representing the sample size and size distribution.

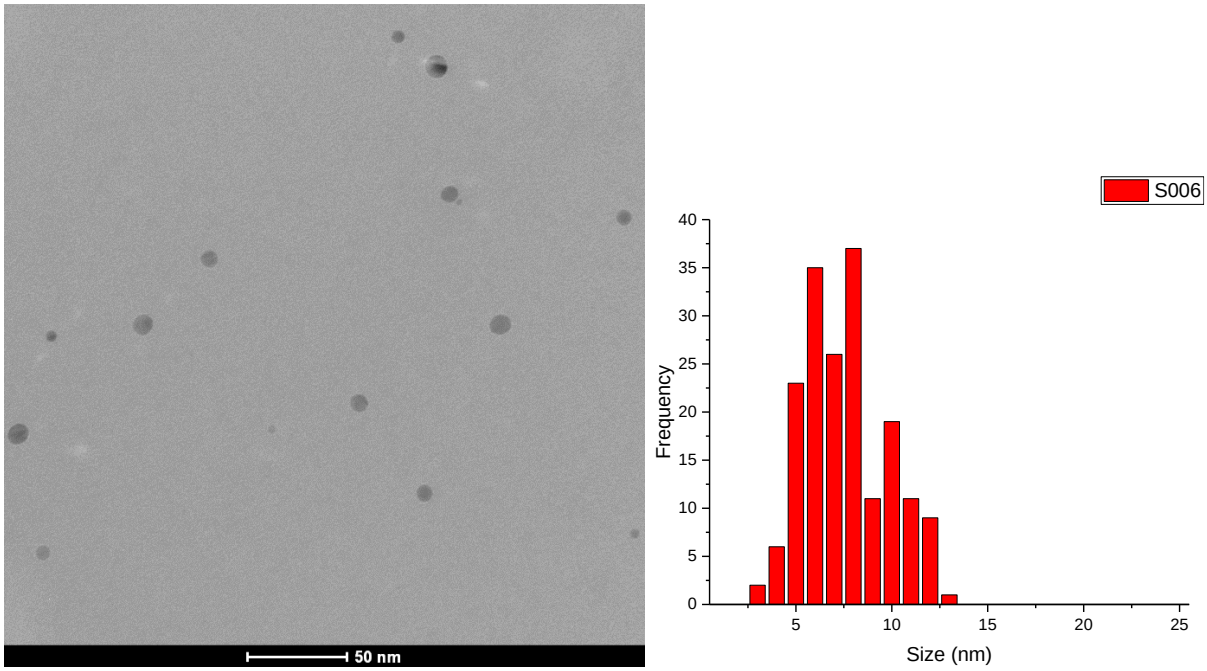

Figure 7: Representative TEM image of the S006 dispersion at the position 1 and the histogram representing the sample size and size distribution.

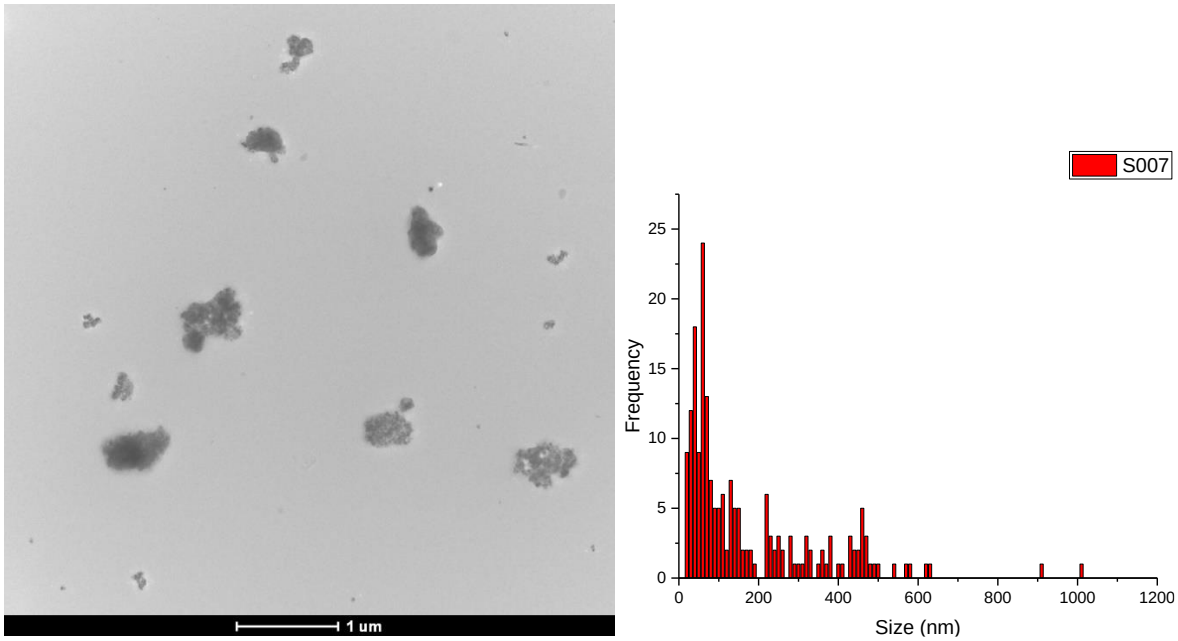

Figure 8: Representative TEM image of the S007 dispersion at the position 1 and the histogram representing the sample size and size distribution.

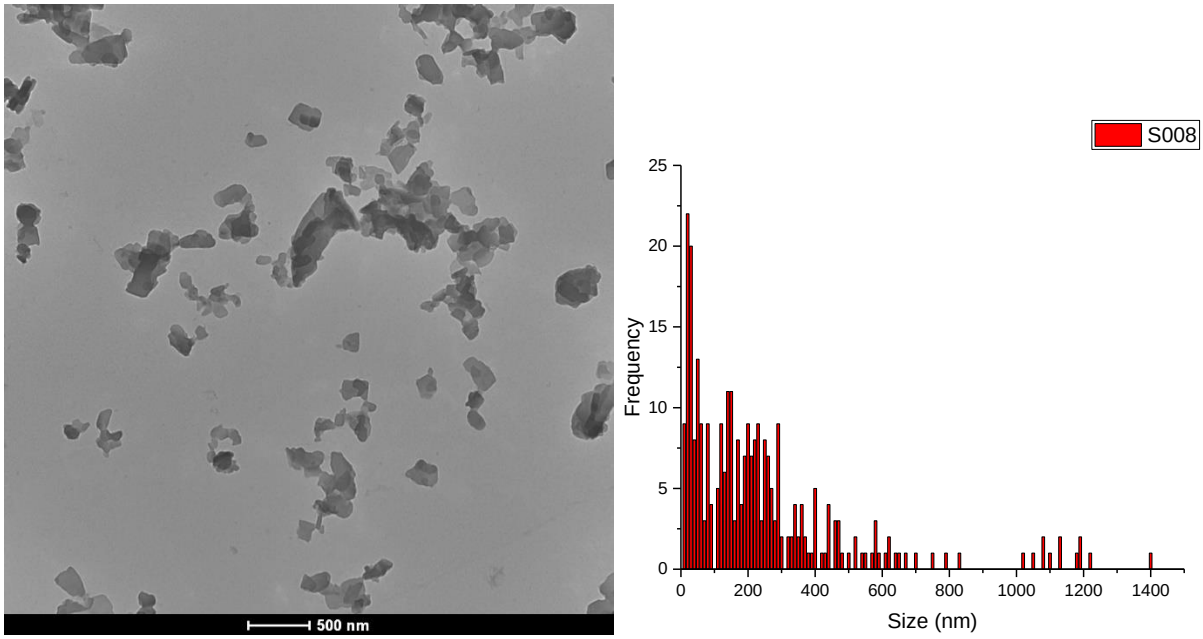

Figure 9: Representative TEM image of the S008 dispersion at the position 1 and the histogram representing the sample size and size distribution.

Dynamic light scattering (DLS) and sizing analysis

Comments:

The DLS measurements were performed by using the NANoREG D2.08 SOP 02 as a guidance and the summary of the characterization is given in Table 3 and Annex I. Due to the fact that most of the samples appeared to be aggregated/agglomerated, the measurements were performed using two instruments for cross-checking results and the resulting sizes are estimated based on the intensity weighted distribution.

Samples S005 and S006, even at the stock solution concentration, showed to be insufficiently concentrated to generate a sufficient scattering profile, which is evident by the low count numbers (reported in Annex I), making the results unreliable. Due to the more powerful laser and consequently higher count number, the analysis done on LS instruments better correlates with the size obtained by TEM.

As for the S001-4 and S007-8, both instruments indicated similar sizes, and the histograms obtained by the Brookhaven indicate sample polydispersity (Figure 10-17), which is in agreement with what is observed in TEM data.

Table 3. DLS sizing - data summary. Top: size obtained with Brookhaven instrument, bottom: size obtained with LS Instruments.

Sample	Average size (nm)	Uncertainty	PDA
S001	395	3.1	0.212
S001	318.8	2.6	
S002	233	4	0.224
S002	210	2.4	
S003	221.9	1.1	0.095
S003	211.2	2.4	
S004	281.9	1.3	0.121
S004	276.4	1.8	
S005	57.9	1.9	0.364
S005	8.8 &175.8	2.6 & 46.8	
S006	31.5	0.4	0.318
S006	20.4	0.2	
S007	252.3	2.8	0.186
S007	231.2	1.2	
S008	210.4	1.5	0.128
S008	197.8	2.4	

Multimodal size distribution graphs obtained by Brookhaven instrument:

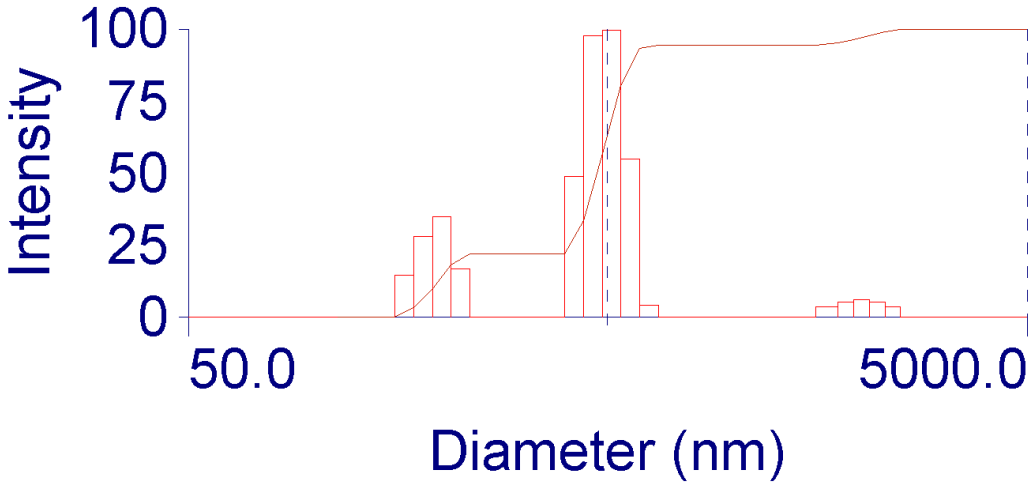

Figure 10: DLS data showing multimodal size distribution for S001.

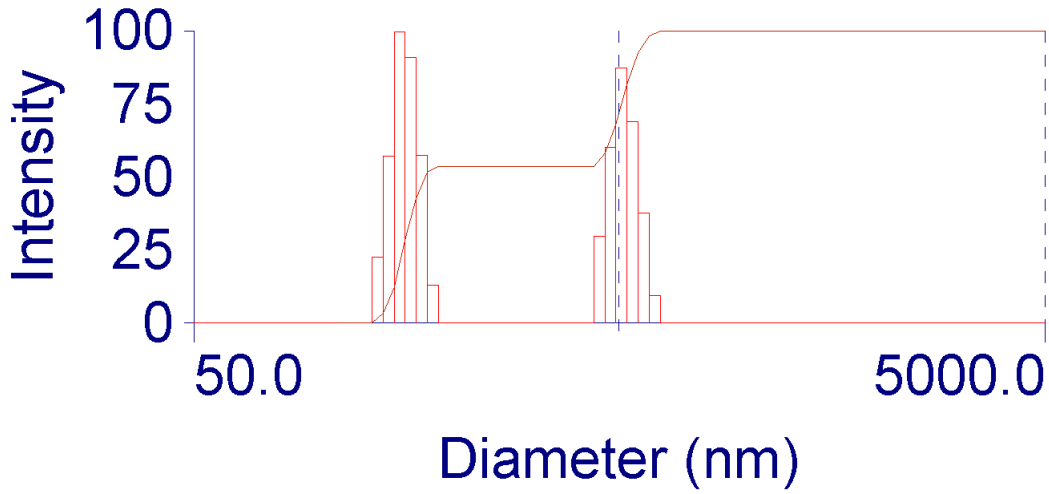

Figure 11: DLS data showing multimodal size distribution for S002.

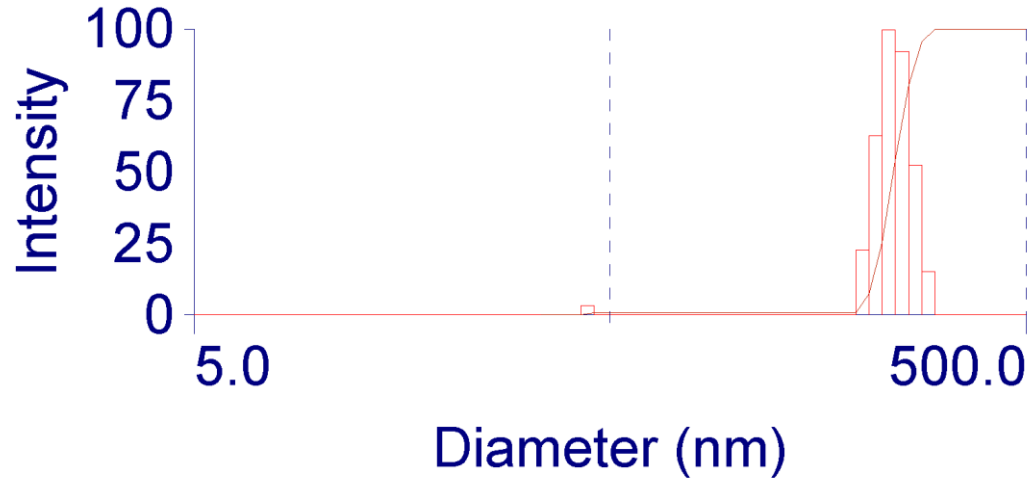

Figure 12: DLS data showing multimodal size distribution for S003.

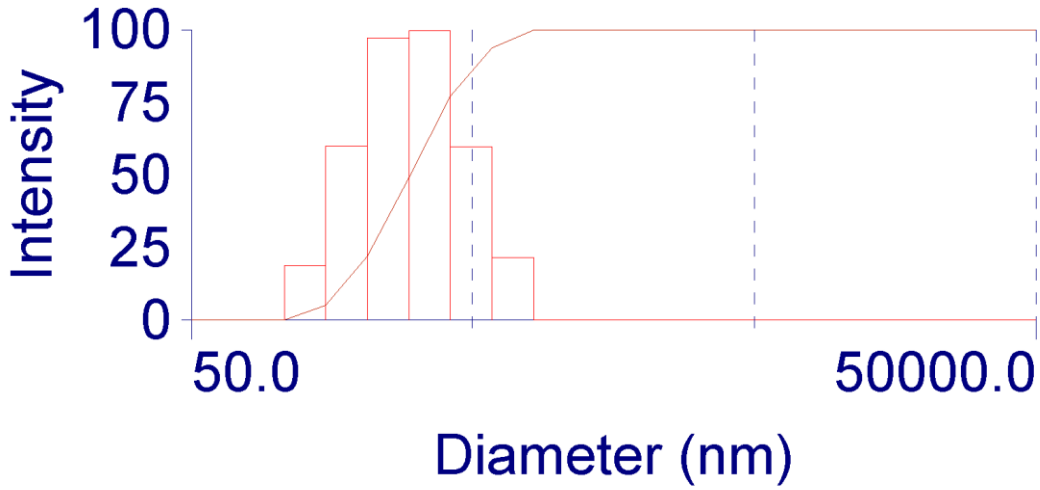

Figure 13: DLS data showing multimodal size distribution for S004.

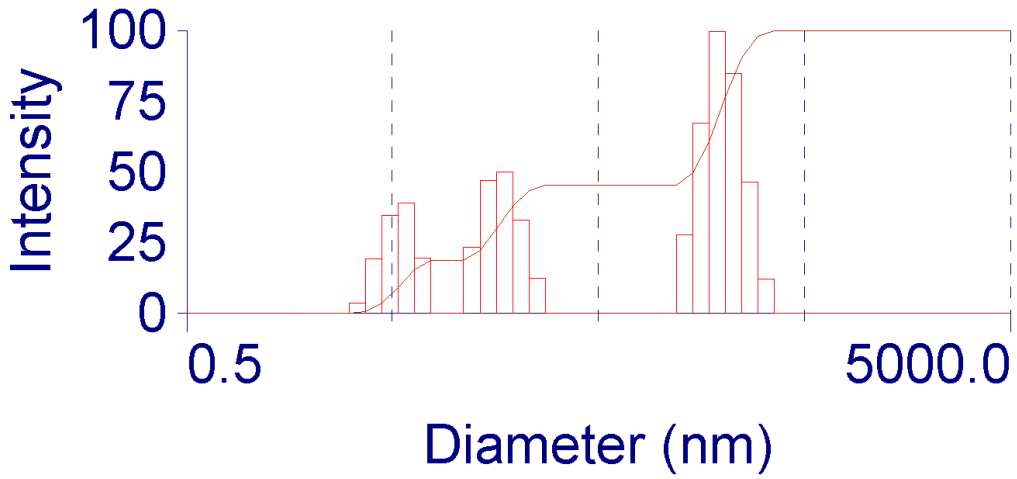

Figure 14: DLS data showing multimodal size distribution for S005.

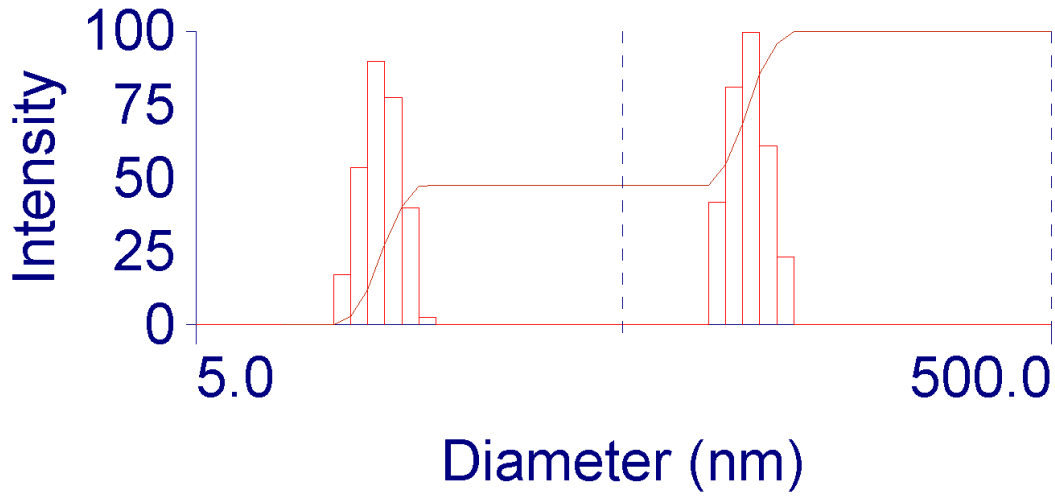

Figure 15: DLS data showing multimodal size distribution for S006.

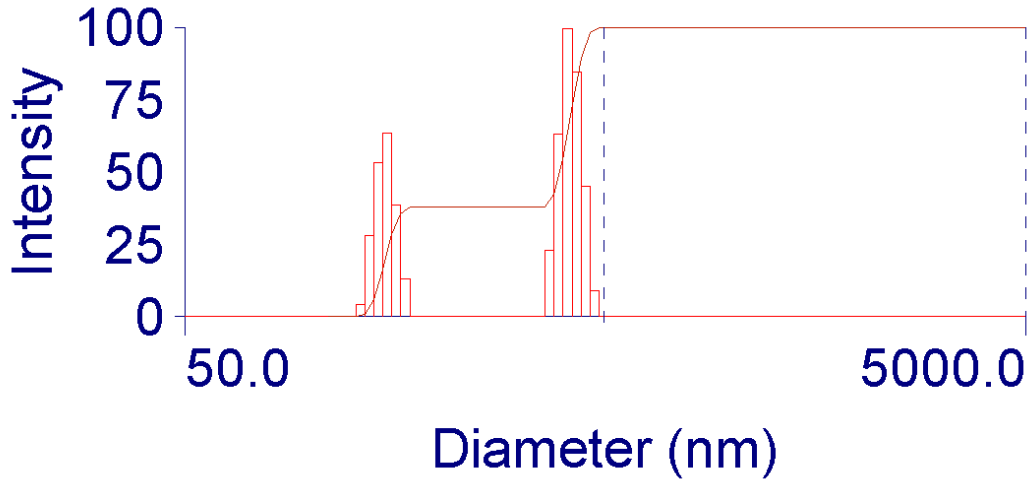

Figure 16: DLS data showing multimodal size distribution for S007.

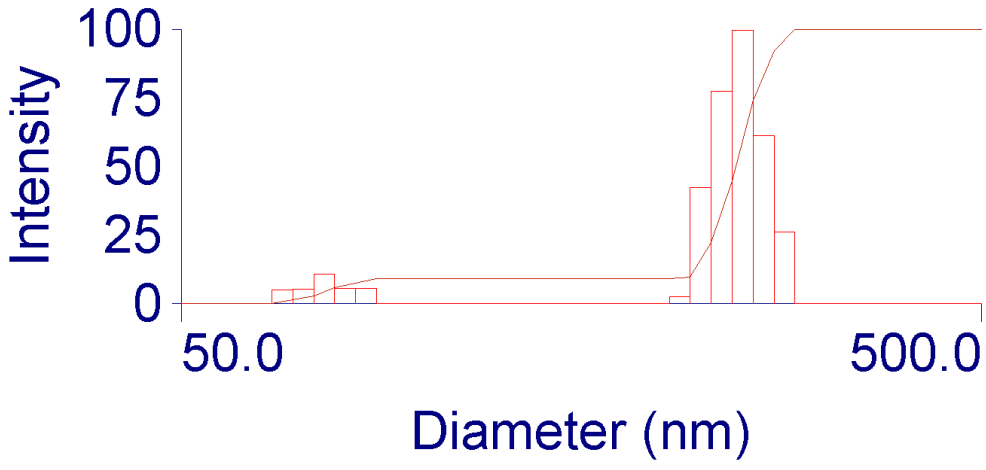

Figure 17: DLS data showing multimodal size distribution for S008.

Dynamic light scattering (DLS) and stability analysis

Comments:

The nanoparticle stability assessment was performed by using the NANoREG D2.08 SOP 02 as a guidance and the summary of the characterization is given in Table 4, Figures 18-33 and Annex I. Due to the fact that most of the samples appeared to be aggregated/agglomerated, measurements were performed at two instruments for cross-checking and to allow for the samples to be measured at 37 °C (LS Instruments).

On average, the nanoparticle sizes increased upon dispersion in cell culture media, which is to be expected due to the likely formation of a protein corona. Such behavior in the case of aggregated/agglomerated samples can not be taken as a rule, since the presence of proteins can lead to the stabilization of smaller agglomerate fractions as well as influence the measurements by the scattering of the proteins themselves.

In some cases, it was indeed observed that the apparent nanoparticle sizes decreased following the 48 h incubation, however based on the data given in Table 3 such a decrease cannot be interpreted as complete re-dispersion of the aggregated/agglomerated samples.

Unfortunately, no reliable results could be obtained for samples S005 and S006 due to their low concentration and hence low scattering. To assess the stability of S005 and S006, based on the shift in the local surface plasmon resonance (LSPR) band, UV Vis measurements were conducted. However, the provided DMEM media caused a strong interference throughout the measured spectra, and although no significant change in the LSPR band was observed for the samples, the measurements should be repeated and performed in a media free of phenol red (Figure 34-38).

For sample S004 (at a concentration 1000x more diluted than the one used for the exposure) an apparent aggregation upon dispersion in the cell culture media was observed. After the 48h incubation, the apparent nanoparticle size decreases, likely due to the protein mediated stabilization.

In conclusion, both instruments provided similar results in particle sizes, and the histograms obtained by the Brookhaven indicated a high sample polydispersity (Figure 18-33), which is in agreement with what is observed in the TEM.

Table 4. DLS sizing - stability data summary. Columns 3-5: results obtained with the Brookhaven instrument, columns 5 and 6: results obtained with LS Instruments.

Sample	**Average size (nm) Brookhaven**	**Uncertainty Brookhaven**	**PDA Brookhaven**	**Average size (nm) LS Instrum.**	**Uncertainty LS Instrum.**
S001 (0 h)	351.6	3.9	0.214	279.8	7.2
S001 (48 h)	266.7	1.8	0.166	315.2	52.6
S002 (0 h)	313.9	6.8	0.213	290.2	6.6
S002 (48 h)	259.7	1.3	0.15	319.2	74.4
S003 (0 h)	302.7	2.6	0.117	264.2	3.4
S003 (48 h)	446.6	5.5	0.304	318.4	18
S004 (0 h)	964.7	18.8	0.156	706.8	18.6
S004 (48 h)	383.5	3.3	0.267	331.2	22
S005 (0 h)	36.5	0.2	0.284	signal too weak	signal too weak
S005 (48 h)	52	0.3	0.293	signal too weak	signal too weak
S006 (0 h)	41.7	0.7	0.288	signal too weak	signal too weak
S006 (48 h)	62.1	0.6	0.232	signal too weak	signal too weak
S007 (0 h)	277.1	5.1	0.13	260.6	5.8
S007 (48 h)	272.7	1.6	0.171	248.2	16.4
S008 (0 h)	246.3	1.5	0.114	228.4	2.2
S008 (48 h)	270.8	1.9	0.157	236.6	17

Multimodal size distribution graphs obtained by Brookhaven instrument:

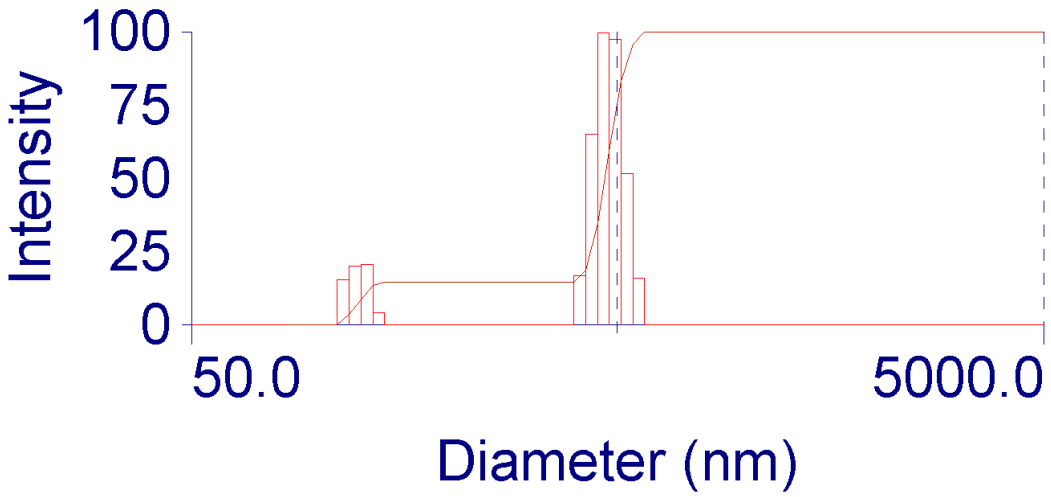

Figure 18: DLS data showing multimodal size distribution for S001 0 h.

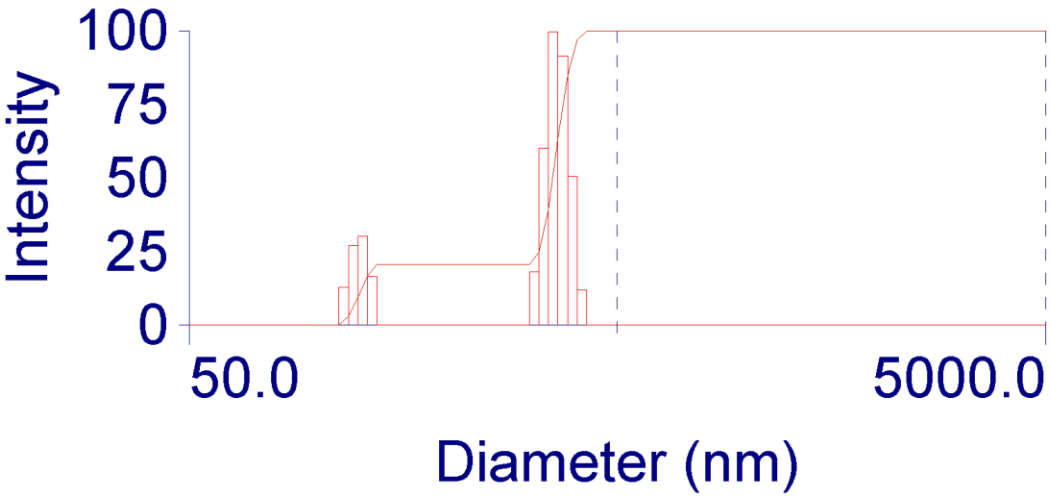

Figure 19: DLS data showing multimodal size distribution for S001 48 h.

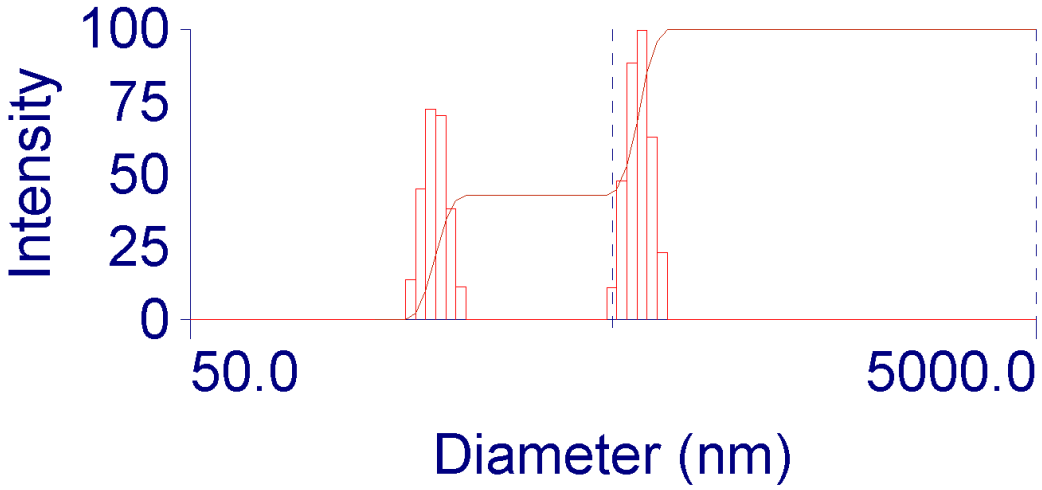

Figure 20: DLS data showing multimodal size distribution for S002 0 h

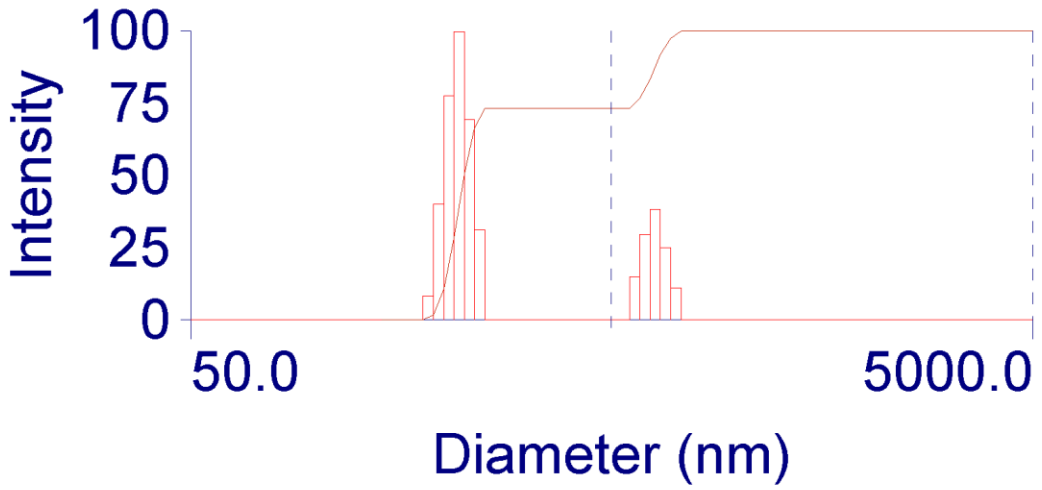

Figure 21: DLS data showing multimodal size distribution for S002 48 h

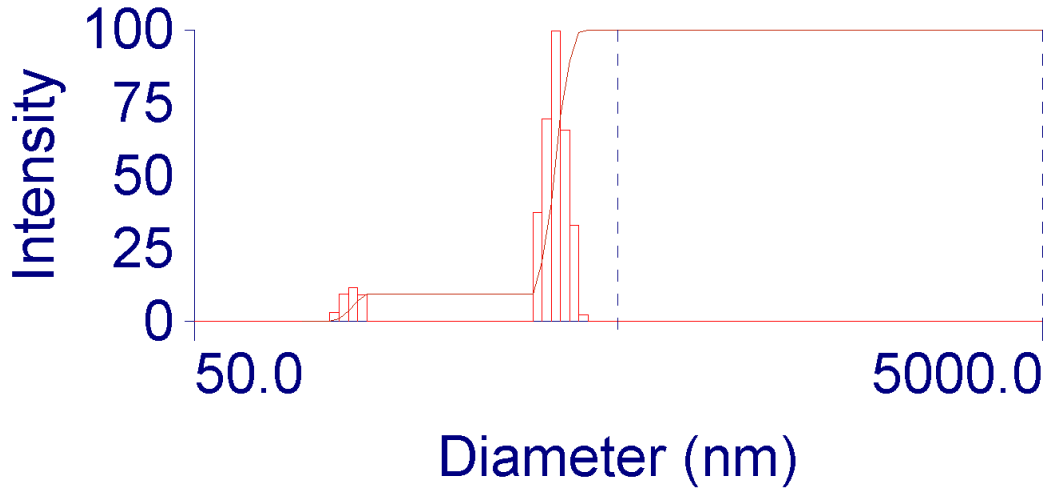

Figure 22: DLS data showing multimodal size distribution for S003 0 h

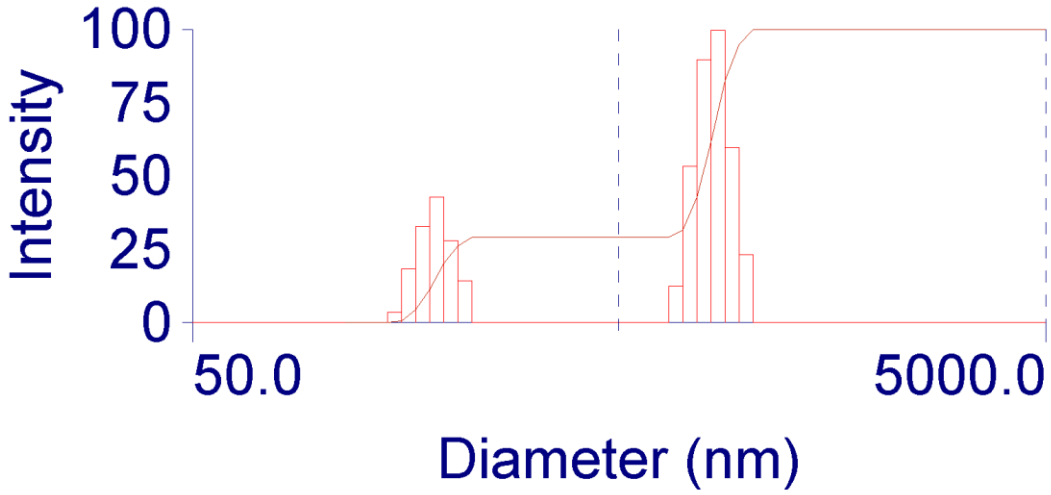

Figure 23: DLS data showing multimodal size distribution for S003 48 h

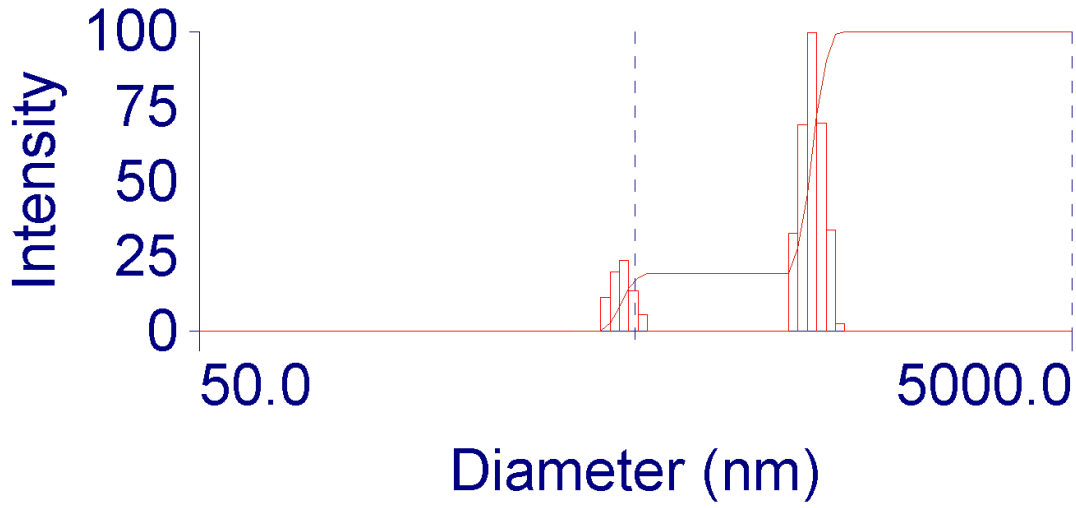

Figure 24: DLS data showing multimodal size distribution for S004 0 h

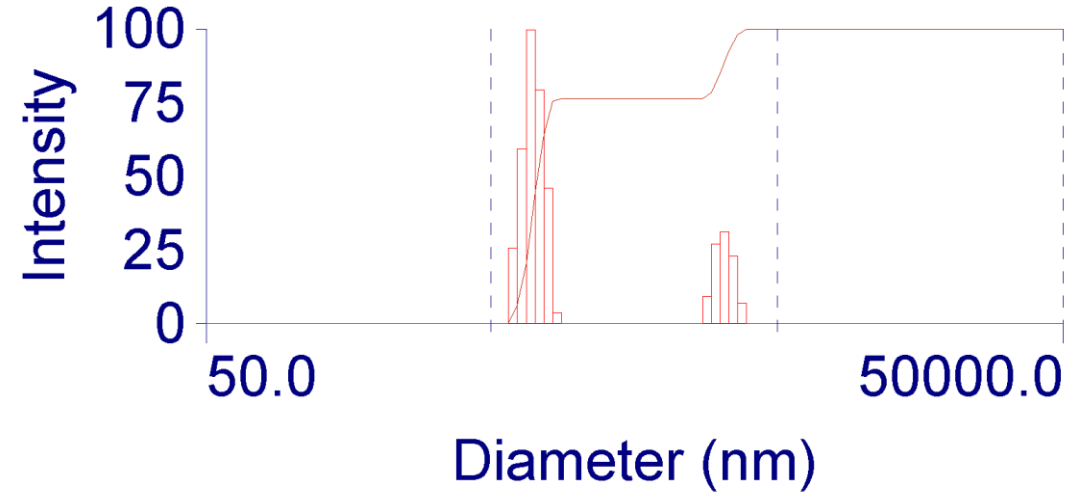

Figure 25: DLS data showing multimodal size distribution for S004 48 h

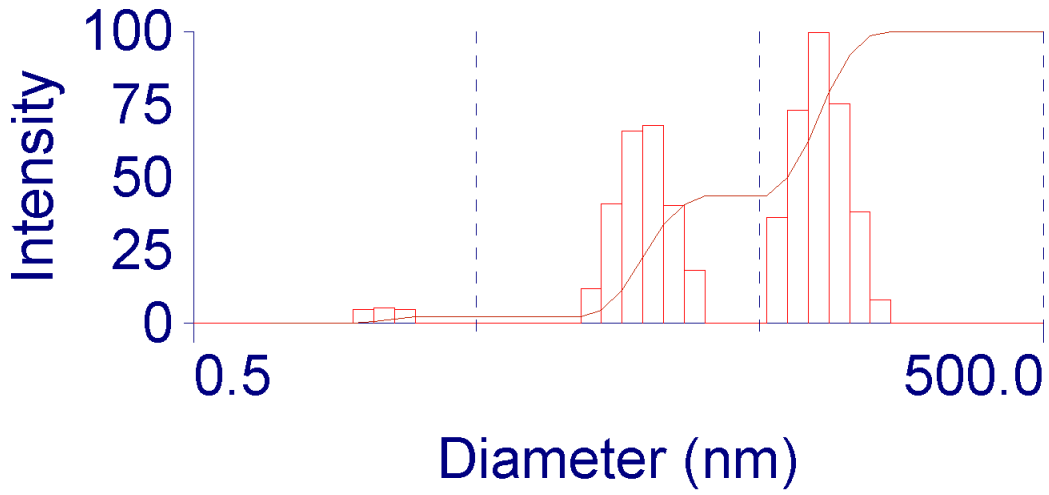

Figure 26: DLS data showing multimodal size distribution for S005 0 h

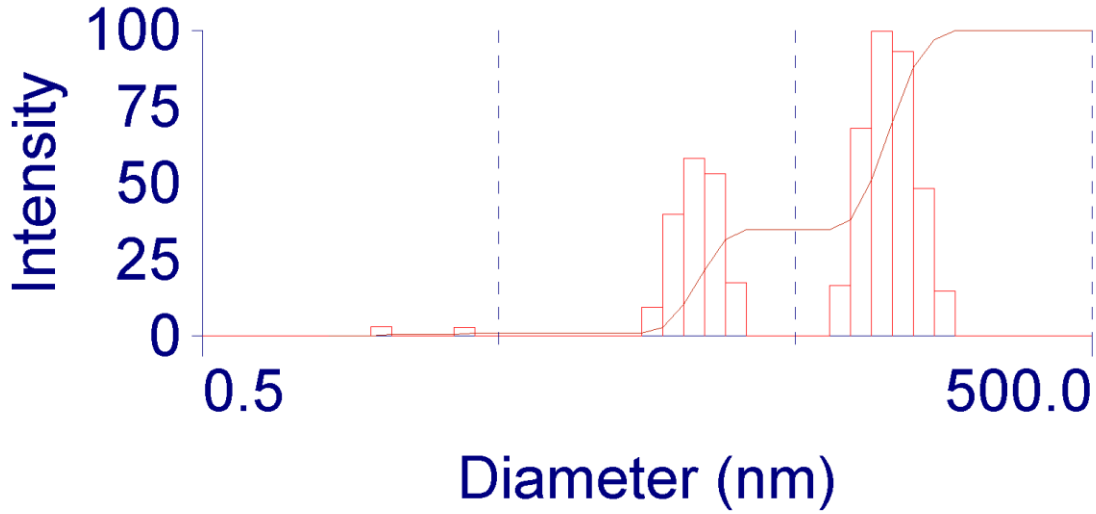

Figure 27: DLS data showing multimodal size distribution for S005 48 h

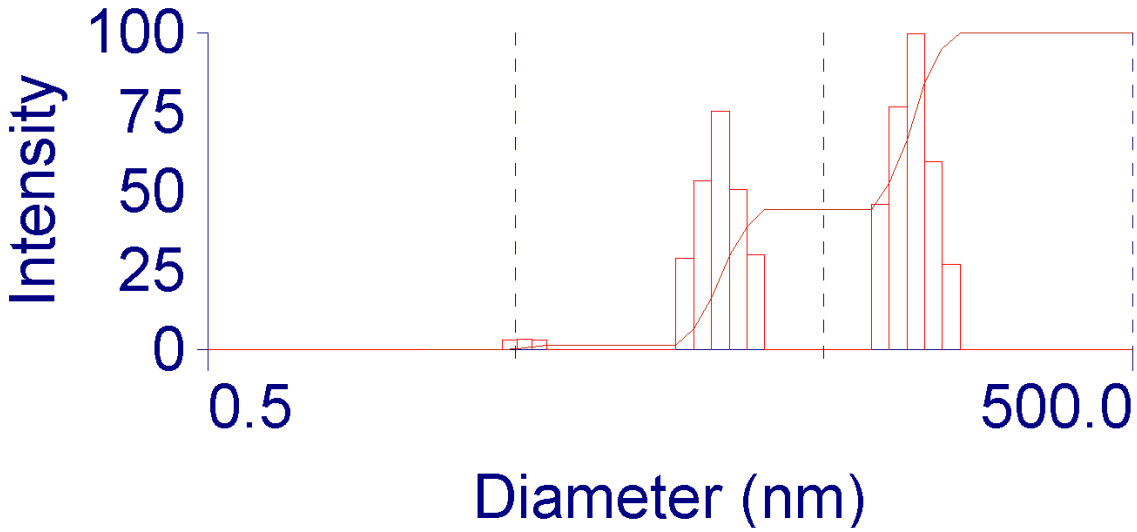

Figure 28: DLS data showing multimodal size distribution for S006 0 h

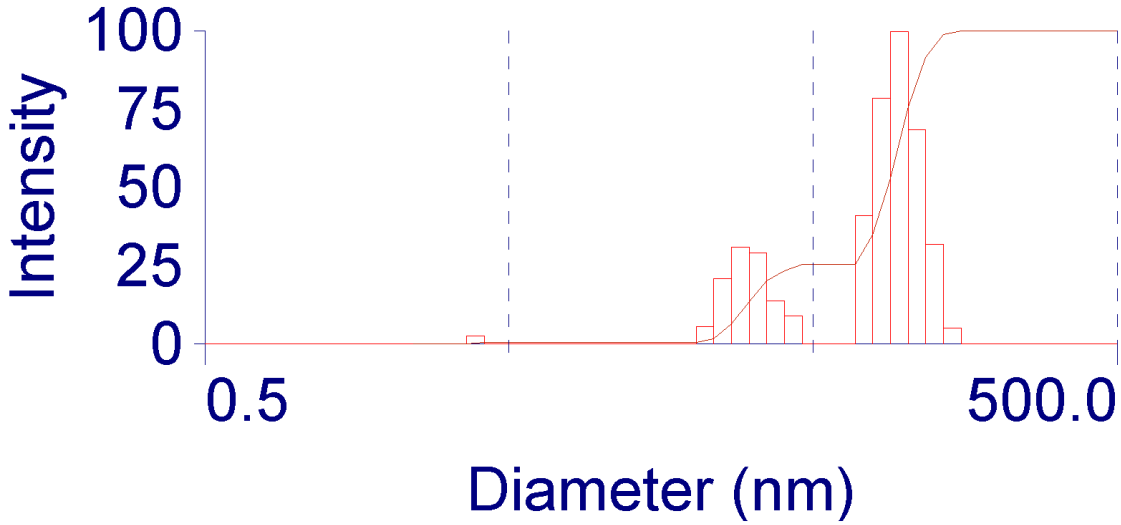

Figure 29: DLS data showing multimodal size distribution for S006 48 h

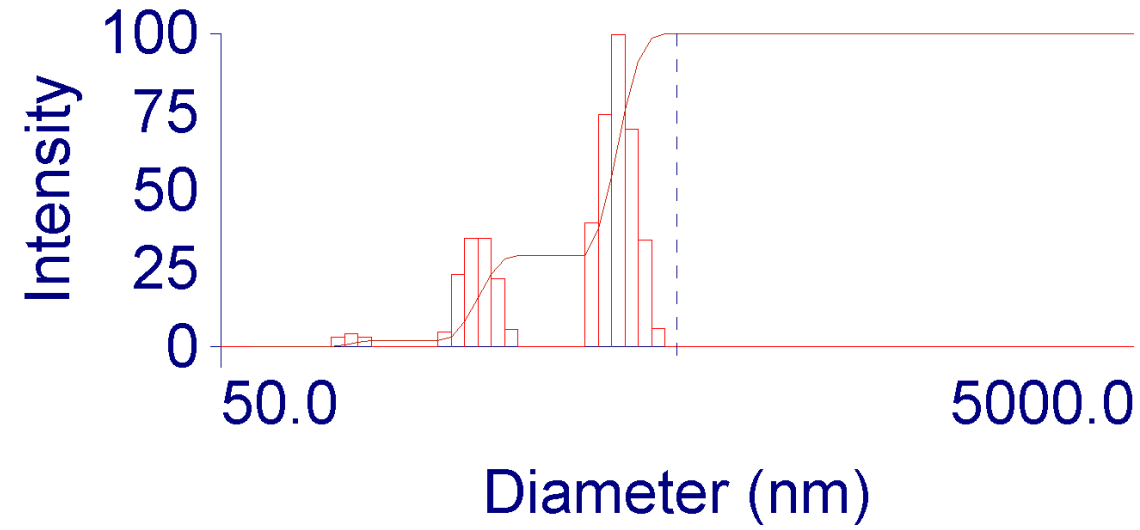

Figure 30: DLS data showing multimodal size distribution for S007 0 h

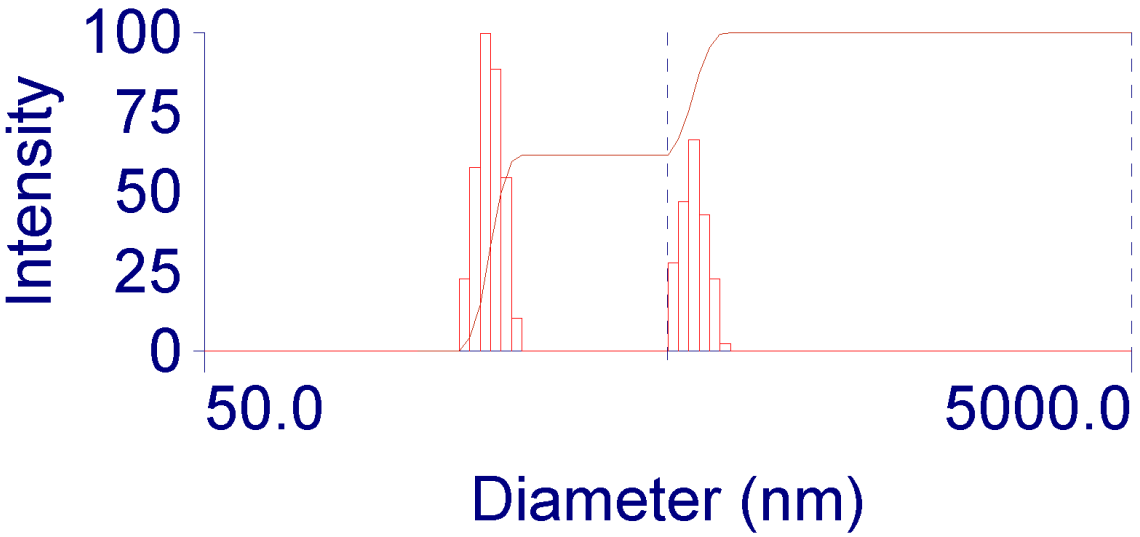

Figure 31: DLS data showing multimodal size distribution for S007 48 h

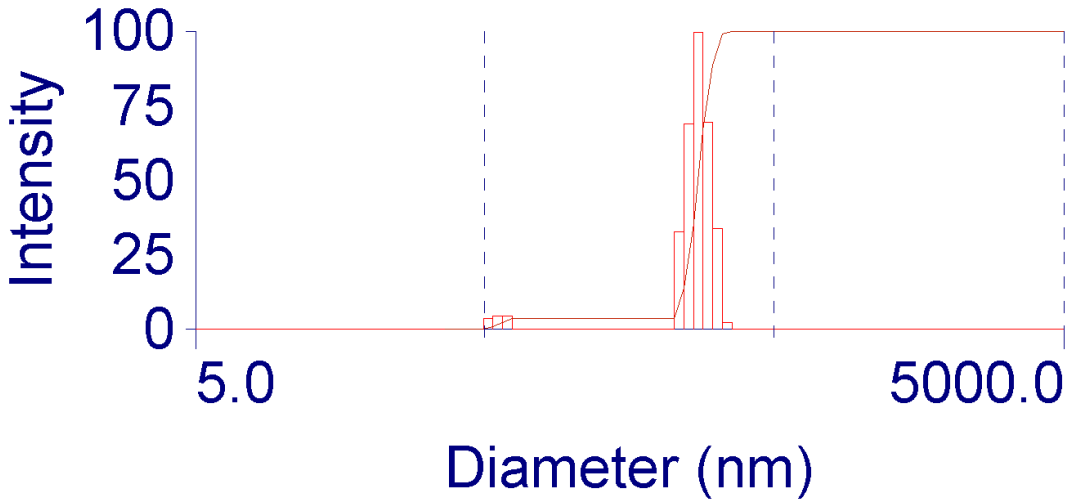

Figure 32: DLS data showing multimodal size distribution for S008 0 h

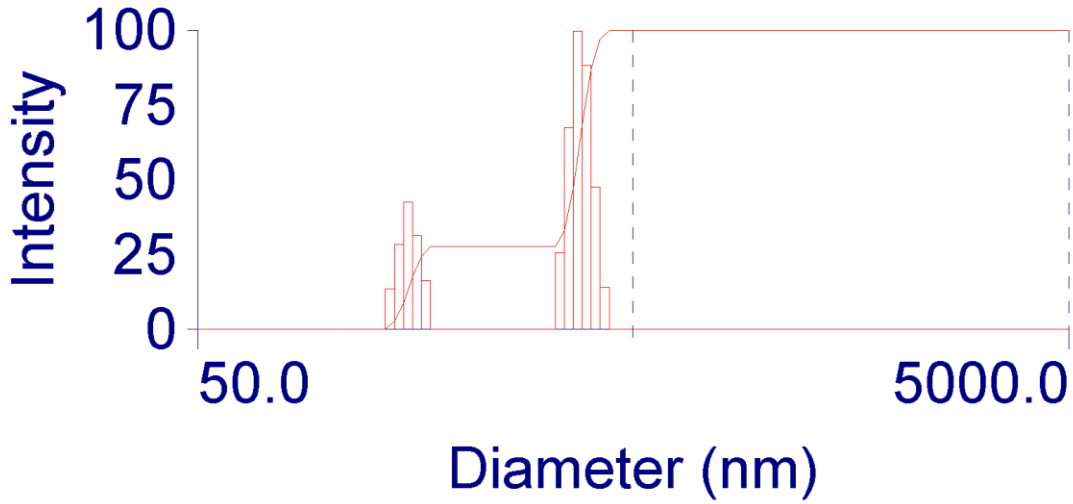

Figure 33: DLS data showing multimodal size distribution for S008 48 h

Assessment of S005 and S006 samples by UV Vis:

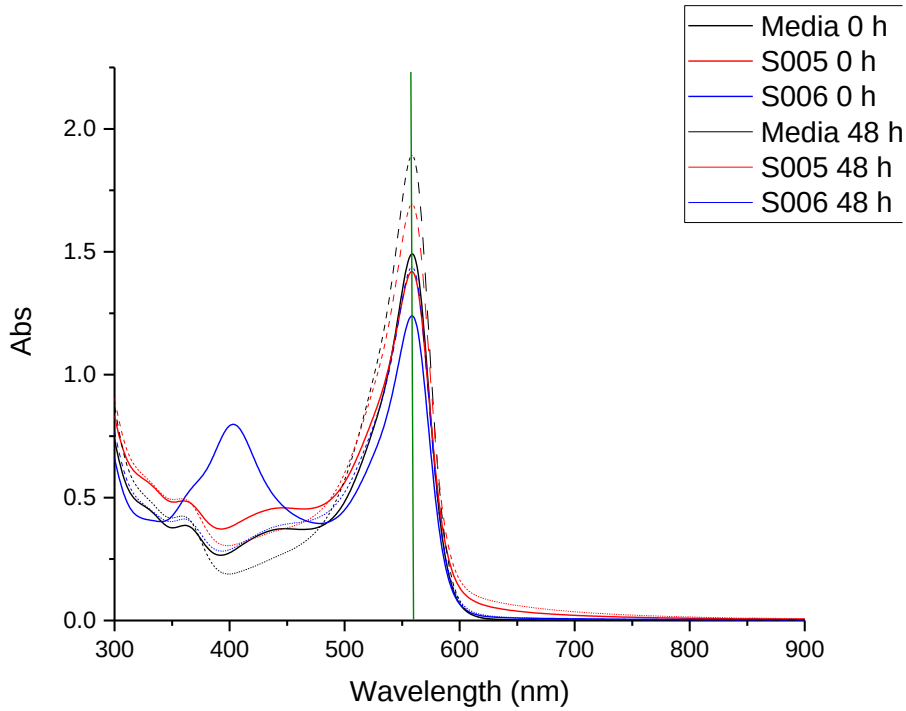

Figure 34: UV Vis data summary showing the spectra of DMEM media, S005 and S006 at the beginning and the end of the incubation

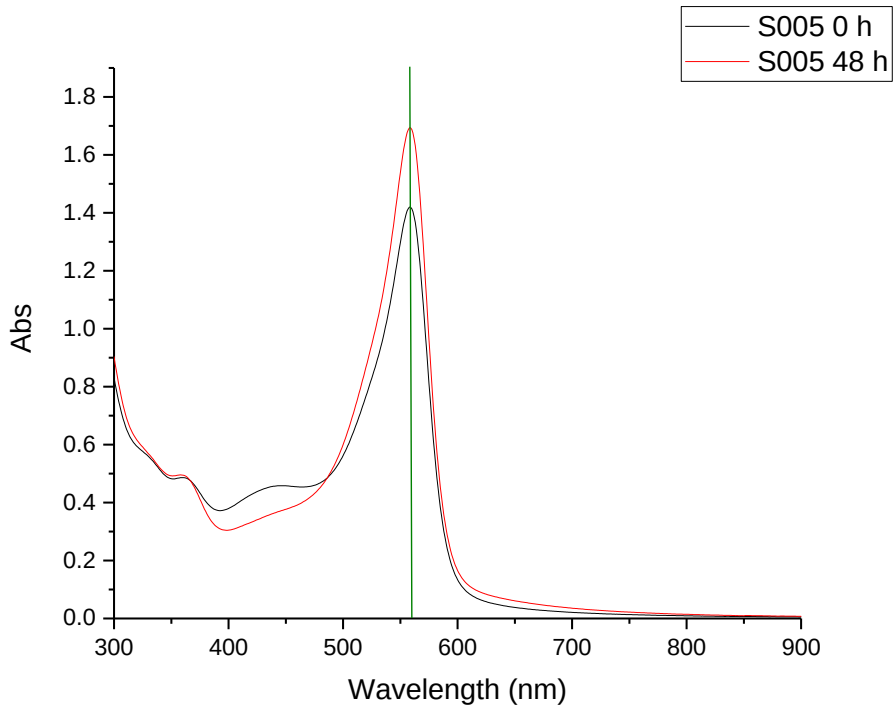

Figure 35: UV Vis data showing the spectra of DS006 at the beginning and the end of the incubation

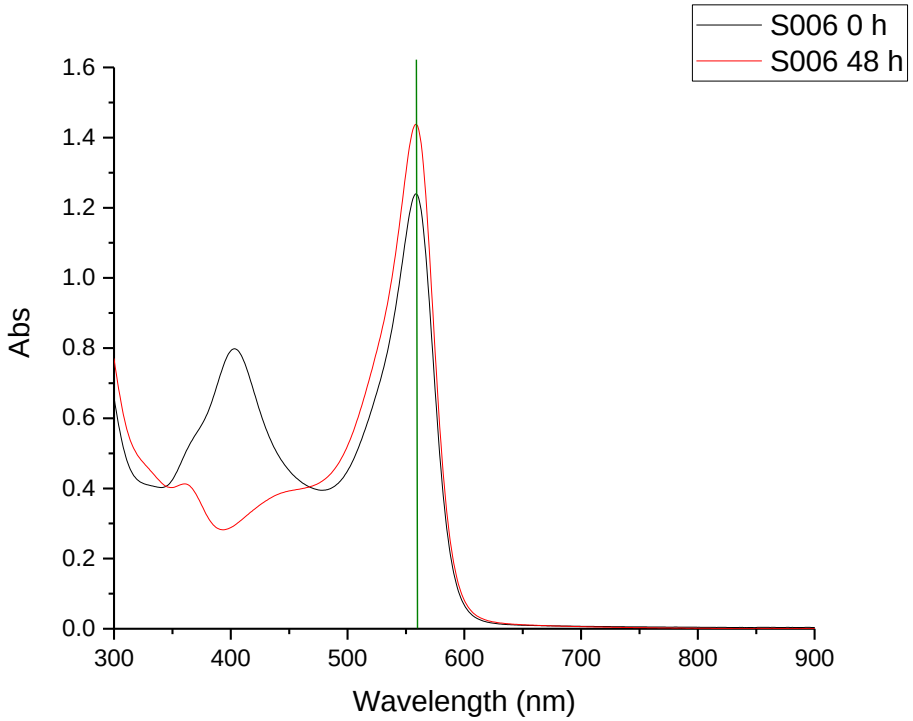

Figure 36: UV Vis data showing the spectra of S006 at the beginning and the end of the incubation

Endotoxin Analysis

Comments:

Both performed assays passed the quality control regarding the linearity of the standard curve, the standard sample accuracy, as well as the sample precision and absorbance interference at 410 nm. For details refer to Annex III and the Sheets: Calibration, Quality control and Absorbance control.

The samples were regarded as endotoxin positive based on the limit given for cell studies - 1 EU/mL (DOI: /10.1016/j.reth.2017.08.004).

Samples S002, S006, S007 and S008 are, according to both assays, under the allowed limit of 1 EU/mL and can be considered as endotoxin negative for cell studies.

The endotoxin assessment for the sample S003 was not in agreement, when comparing both assays (2.55 EU/mL for LAL Pierce assay and < 1 EU/mL for Endosafe® nexgen-PTS™). In any case these results cannot be regarded as reliable as the sample showed significant interference with the signal i.e. inhibition.

Sample S004, although showing inhibitory behaviour in the LAL Pierce assay, at a 100x dilution did not show the same behaviour for the Endosafe® nexgen-PTS™ assay, and the obtained value < 1 EU/mL can be seen as reliable.

Sample S001 did not show any interference and when tested with the Endosafe® nexgen-PTS™ assay, showed a positive value just above the 1 EU/mL threshold

Sample S005 showed a strong positive value in both assays but the Endosafe® nexgen-PTS™ assay showed significant interference, in this case enhancement, which renders this result unreliable.

In order to make a definitive statement on the presence of endotoxins in the samples (> 1 EU/mL), ideally the samples (specifically S003, S004 and S005) would have to be tested with additional assays e.g. TLR4 reporter cells (DOI: 10.1186/1743-8977-9-41).

Sample	Full Name	Pierce Assay	PASS/FAIL + reason	Endosafe	PASS/FAIL + reason	Comments
S001	Nickel NPs	0.15	PASS	**< 1.31**	PASS	Very low amount detected via only one assay- 3rd assay is needed for clarification
S002	Titania NPs	0.05	PASS	< 1	PASS	Double negative - reliable result
S003	Tattoo ink black	**2.55**	FAIL quality control/ inhibition	< 1	FAIL quality control/ inhibition	Inconclusive due to the quality control fail in both assays
S004	Tattoo ink black	0.21	FAIL quality control/ inhibition	< 1	PASS	Negative result according to Endosafe assay
S005	Gold NPs	**15.86**	PASS	**< 51.6**	FAIL quality control/ enhancement	Pierce assay - positive, Endosafe - positive but fail due to the signal enhancement
S006	Silver NPs	0.32	PASS	< 1	PASS	Double negative - reliable result
S007	Titania NPs	0.079	PASS	< 1	PASS	Double negative - reliable result
S008	Tattoo ink red	0.34	PASS	< 1	PASS	Double negative - reliable result

Analysis Summary

When possible, the sample measurements and the analysis were performed according to NANoREG SOPs. The sizing and stability measurements were significantly impacted by not achieving a high quality of dispersion (i.e. samples showing large size distribution and large aggregated and samples showing sedimentation), following the defined dispersion protocol. The optimization of the dispersion protocol should be considered, to achieve more accurate and reliable size and stability information.

Furthermore, due to their nature, samples interfered with the endotoxin assessment. S005 proved to be a critical sample and it should be confirmed as positive via additional above-mentioned assays.